Rethinking of buckling bars via resonances
Literature review

Jialun Liu
(under supervision of Dr. Ralph Schönrich)

28 October 2020

Department of Physics and Astronomy
University College London

CONTENTS

ABSTRACT

Our Milky Way's (MW) bar has a boxy-peanut (BP) shape, characterised by a central X-shaped structure. The project aims to understand the involvement of vertical Lindblad resonances (VLR) in the buckling of a galactic bar. We are particularly interested in the effect that a slowing bar (responsible for changing the horizontal frequencies) might have brought to the vertical motion of resonant stars. If we can establish a firm connection, we will solidify our understanding of how and why these BP/X-shaped bars develop.

1. INTRODUCTION

Most disc galaxies exhibit a central bulge which presents itself in three ways: **(1)** classical bulges are distinct with their spherical shapes which are consist of kinematically hot old stellar populations (Brooks and Christensen, 2016); **(2)** pseudo-bulges that possess disc-like structures where young, metal-rich stars are populated, constructed under the influence of the embedded bars (Kormendy et al., 2004); **(3)** BP/X bulges/bars demonstrate the shapes when viewed from side-on. Like the MW, nearly half of external disc galaxies have now been observed to own BP/X structures (Shaw, 1987; Combes et al., 1990; Laurikainen et al., 2011). This type of bulge is well confirmed to be the thicker component of the strong galactic bars (Bureau et al., 2006; Erwin and Debattista, 2013) which arise from the instability of the disc. Located in the galactic centre as always, a bar is a flat elongated component often regarded as a rotating rigid body with a steady pattern speed (Binney and Tremaine, 2008). Many studies have proven that a galactic bar grows in size by exchanging the angular momentum from its inner disc to outer discs and dark matter halos (Athanassoula, 2003). As it thickens and slows down (Aumer and Schönrich, 2015; Chiba et al., 2019), the bar bends the stars' orbits out of the disc plane under three main mechanisms, namely, **buckling instability** (Toomre, 1966; Combes et al., 1990) (see section 2.2), **resonance sweeping** (Weinberg, 1985) and **resonance capturing** (Quillen, 2002) (See both in section 2.3). The BP/X-shaped bar in the MW is either formed through one or a combination of these processes.

A central galactic bar plays an essential role in the dynamical evolution of a galaxy: its presence might affect the star formation rates (Hawarden et al., 1986; Hummel et al., 1990), spatial star formation patterns and overall metallicity contents (Friedli et al., 1994; Vera et al., 2016). The relation between stellar populations within the bar and the bar thickening process is still obscure. Hence, understanding the bar formation enables us to interpret the evolutionary history of the MW. More importantly, comparing the MW with other disc galaxies broadens our horizons with the kinematic structure of the external galaxies.

The following literature review consists of information regarding the observational discovery of BP/X-shaped bars (section 2.1), elaboration and comparison of three theoretical models related to the phenomenon (section 2.2 & 2.3), a further discussion concerning the shapes of BP/X orbits (section 2.4), and a final outline detailing the project's tasks and deadlines (section 3).

2. BACKGROUND

2.1. Observational evidence

Two infrared/microwave surveys, COBE (Dwek et al., 1995) and 2MASS (Skrutskie et al., 2006), are famous for their clear and detailed mappings of BP-shaped bars in the MW centre (Freudenreich, 1998). This is because the galactic dust covering the MW's central region becomes transparent when viewed at longer wavelengths, such as infrared and microwave. Following their success, advancements in observational technology have allowed for techniques such as OGLE (Nataf and Udalski, 2010), that were developed for image detection and analysis within a satellite. In 2010, McWilliam and Zoccali (2010) interpreted the X-shaped structure from the split of red clump stars in the MW bar. The two equally populated peaks in the density distribution indicate the existence of two populations of stars that forms an X shape (McWilliam and Zoccali, 2010; Nataf et al., 2010). This idea was validated by the VVV survey (Wegg and Gerhard, 2013) and the three dimensional (3D) kinematics of our galactic bar has been studied and compared in greater detail by Vásquez et al. (2013). The clearest morphological X-shaped bar image of our MW is on the right panel of Figure 2.1, achieved by Ness and Lang (2016). WISE, an Infrared telescope, was launched to conduct a full-sky photometric survey (Wright et al., 2010) in the central region of the MW. The X-shaped structure was extracted computationally by filtering the raw measurements (left panel of Figure 2.1) with an exponential disc model (The middle graph in Figure 2.1). This process is referred to as the unsharp-masking technique. As a result, the X morphology is a consequence of BP-shaped bar withdrawn the median filter (Bureau et al., 2006).

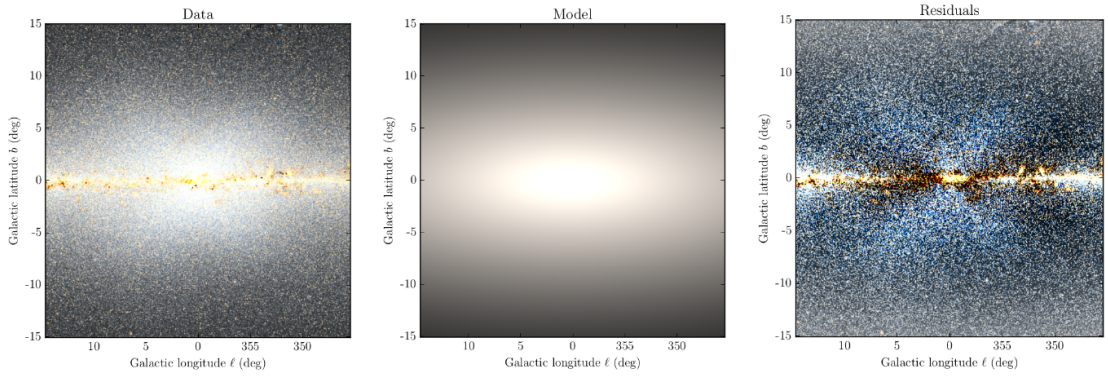

Figure 2.1: Raw data (left); an exponential disc model (middle); residue (right) from Ness and Lang (2016).

More external galaxies with BP/X-shaped morphology were studied and compared with the MW, to develop a better understanding of the MW evolution in addition to the nature of this morphology. For instance, NGC 4710, an external galaxy has been observed to manifest a BP-shaped bar like the MW. Both stellar kinematics and population analysis revealed a missing structural component outside of its bar area compared to the MW (Gonzalez et al., 2016). The additional component present in the MW is a region comprising the oldest and metal-poor stars (Gonzalez et al., 2016), implying the oldest stars in the MW did not evolve with its BP/X-shaped bar. Despite the close resemblance between the two galaxies, the experimental aspects concerning this additional component in the MW still require comprehensive development. For the theoretical model of BP/X structure to be improved, it is therefore evident that further observational data and comparisons with a multitude of external galaxies be executed. In the next sections, theories for solving the bar thickening issue will be discussed.

2.2. Buckling instability

Toomre (1966) studied the dynamics of a three dimensional (3D) thin and pressure-free disc, and noticed the occurrence of buckling instability which destabilizes and thickens the disc. The rise of such instability is a result of coupled motions in radial and vertical components of the disc. In mathematical expressions, σ_z^2/σ_r^2, the ratio of vertical to radial squared velocity dispersion, measures the extent of the buckling instability. Toomre predicted the buckling when this value is below 0.1, however, it was later corrected to be under 0.4 by Sellwood (1996).
In the past 30 years, this theory has been frequently applied and further developed, on account of its potential to solve the bar thickening issue. To illustrate, a growing young bar weakens in strength rapidly and increases its thickness when buckling takes place in the vertical axis. Most importantly, the vertical symmetry of the bar breaks (Martinez-Valpuesta et al., 2006) and forms a “W” shape from side-on, depicted in the mid-row of Figure 2.2. Subsequently, a peanut shape forms when the thickened bar regains its vertical symmetry. The whole peanut shape formation process takes 0.2 Gyr which is short compared to the life of a bar. Moreover, there is a sharp decrease in bar’s strength throughout the process (Martinez-Valpuesta and Shlosman, 2004). Initially, the bar’s in-plane potential is reduced when stars are ejected from the plane after the buckling. Subsequently, the bar loses weakly bound in-plane stars to further weaken its strength.

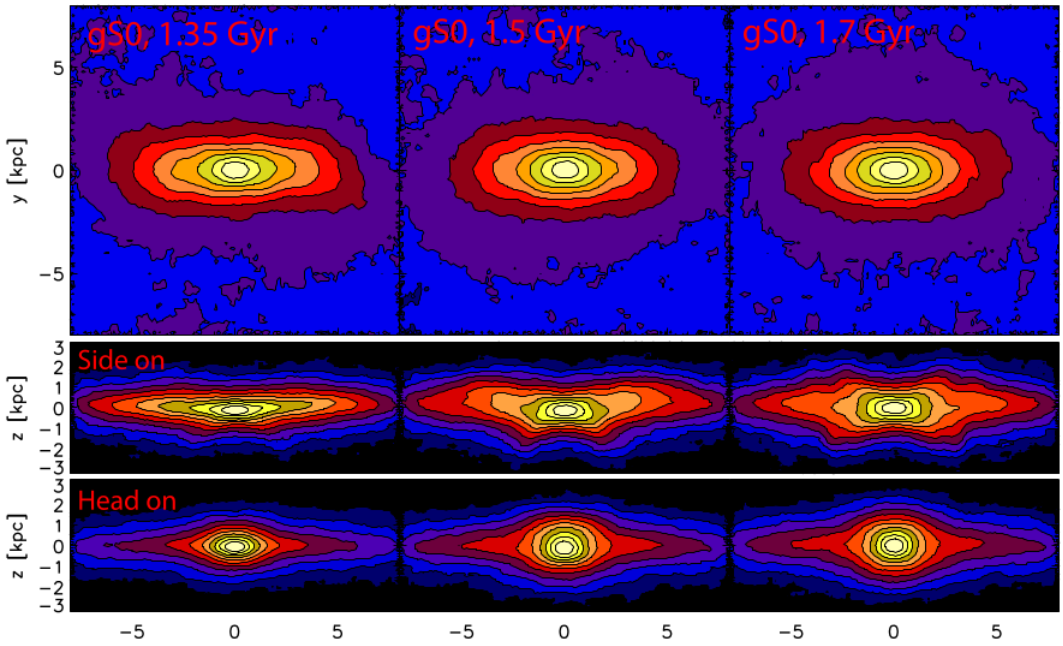

Figure 2.2: Density profiles of a bar undergoes a thickening mechanism throughout a period of 1.7 Gyr. The snapshots are taken at 1.35 Gyr, 1.5 Gyr and 1.7 Gyr in three different angles from Quillen et al. (2014).

However, buckling instability has limitations to explain thickening issues. **(1)** The bar formation rate in this model is rather high, thus it is inadequate to explain the slow formation phenomenon. **(2)** Buckling happens under a strict condition, on a flattened and elongated bar. This condition is not full-filled in the recurrent buckling process (Martinez-Valpuesta and Shlosman, 2004) where the buckling takes place multiple times on a non-flat bar. Hence, this model might explain some galaxies like NGC 3227 and NGC 4569 (Erwin and Debattista, 2016), but alternative mechanisms are required to analyse the bar formations of more disc galaxies.

2.3. Theories of resonances

Proposed by Combes and Sanders (1981) and further developed in Combes et al. (1990); Pfenniger and Friedli (1991); Patsis and Athanassoula (2002a), a key player for the formation of BP/X-shaped stars is resonance. In this model, the bar gets thicker gradually with a perfect vertical symmetry. The vertical density profile (mid-row of Figure 2.3) demonstrates the persistence of the peanut shape. Consistent with the results from Friedli and Pfenniger (1990), buckling instability is not involved in the process and hence not a necessary condition for the bar to thicken. In comparison to the violent buckling instability, this theory undergoes a gentle and stable thickening process.

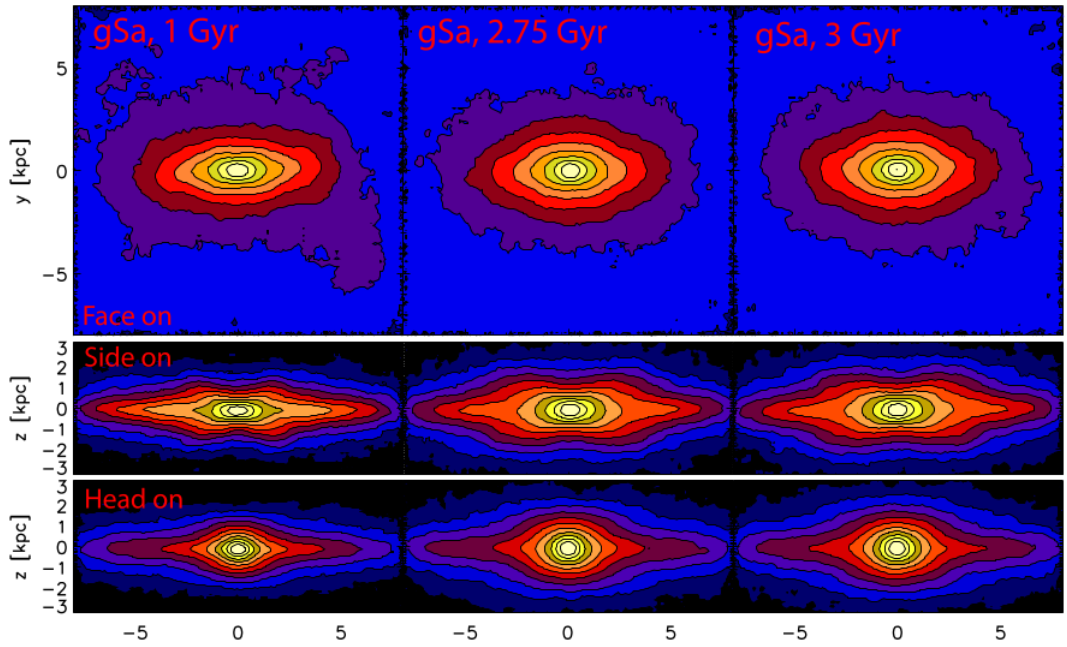

Figure 2.3: The same description as in Figure 3.1. The snapshots are taken at 1Gyr, 2.75Gyr and 3Gyr from Quillen et al. (2014).

However, the underlying mechanism was still poorly understood. After decades of research, two types of resonance were shown to be relevant in such cause; Lindblad resonances and mean-orbit resonances (MOR). The Lindblad resonance can be regarded as the resonance of the bar due to its self-rotations. The bar thickening processes is mainly caused by the 2:1 VLR, with two vertical oscillations per rotation of the bar, $\Omega_x : \Omega_z = 1 : 2$. The MOR describes the orbital resonances of stars and occurs when the ratio between the radial and vertical oscillation frequencies is an integer number. It is mathematically defined as $f_x : f_y : f_z = l : m : n$ (where l, m, n are integers), according to the notation from Sellwood and Wilkinson (1993). Meanwhile, the theory of resonance has evolved into two mechanisms; resonance sweeping and capturing. Both resonance theories have adapted the mathematical model from the levitation mechanism (Sridhar and Touma, 1996), which explained the heated/thickened disc as a consequence of the levitation of stellar orbits.

The resonant sweeping model (Weinberg, 1985; Hernquist and Weinberg, 1992; Quillen et al., 2014) predicts the resonance to sweep through the disc as the bar slows down and grows thicker. The bar can be regarded as a decelerated rotating carousel that spins out its stars. Once a star's orbit begins to resonate, it will be pushed further above the plane of the disc and become part of the BP/X morphology. When the BP/X structure moves outwards via forming new resonant orbits, old ones will be detached and pertain their original trajectories. This mechanism was mathematically devised from a perturbed axisymmetric Hamiltonian from a non-axisymmetric bar (Contopoulos and Weinberg, 1975) and computationally examined by Sellwood and Gerhard (2020). In Figure 2.4, x_{max} gradually deviates from the bar's centre when the time passes by; at a given time, the stars' orbits enlarge their vertical oscillation ranges (z_{max}) in the resonance. This is strong evidence for the radially growing bar when the resonance is swept outwards.

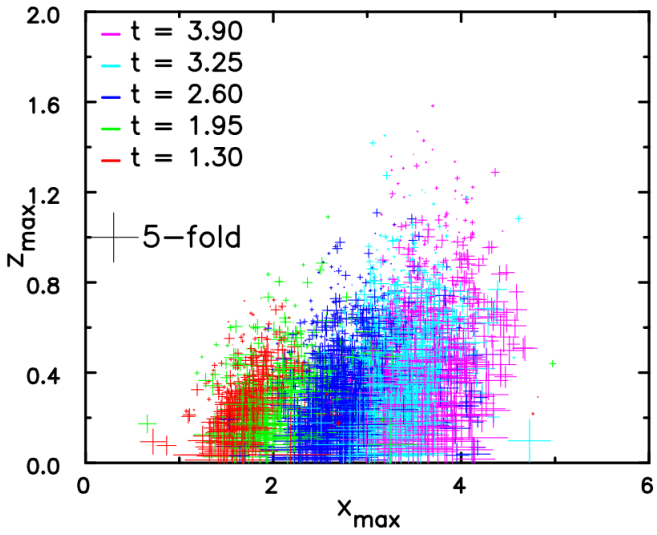

Figure 2.4: Resonant stars' orbits in the x_{max}, z_{max} plane at five different times, t = 1.3, 1.95 2.60, 3.25, 3.90 (Gyr) from Sellwood and Gerhard (2020).

Resonance capturing from Quillen (2002), predicts a vertical growth of the bar if stellar orbits are trapped by the 2:1 VLR. Precisely, when the stars are caught by the resonant motion of an evolving bar, the orbits of stars will levitate over the mid-plane of the galaxy to broaden their vertical oscillation ranges. This mathematical model was later simulated and proven by Sellwood and Gerhard (2020) using N-body simulations (Pfenniger and Friedli, 1991). The orbits of stars that are caught by the resonance of the bar will remain until simulation completion, while simultaneously the bar thickens significantly. However, the orbits that have off-resonance behaviours do not contribute to the thickening process.
Although both theories arise from the 2:1 VLR from the bar, the differences between them are obvious. **(1)** The resonance width in the resonance capturing is narrow (Quillen, 2002), so that the thickened region on the bar might be too small to match up with the actual size of the BP/X-shaped bars from the observational data. **(2)** Resonance capturing will result in a higher stellar density in the inner bar due to the angular momentum loss of the stars' orbits from the inner bar to the outer halo. In Figure 2.5, the right plot's vertex is noticeably narrower and taller than that of the left.

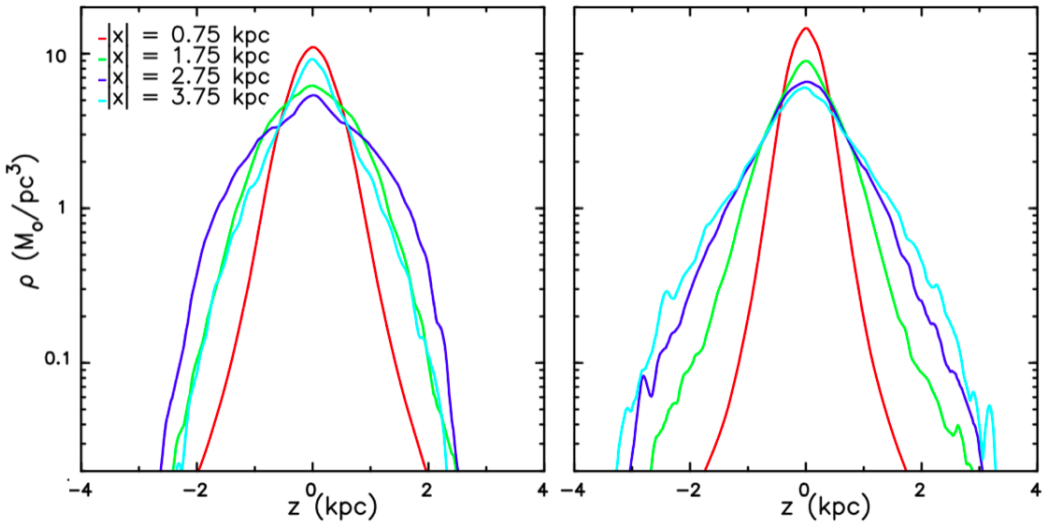

Figure 2.5: The vertical density distributions at varying distances across the bars by the end of the resonance sweeping (left) & capturing (right) simulations. The radial distances are 0.75, 1.75, 2.75, 3.75 (kpc) respectively. Adapted from Sellwood and Gerhard (2020).

2.4. Orbit classifications

A natural question that arises at this stage, what is responsible for the BP/X shapes? A collection of 3D orbits (Pfenniger and Friedli, 1991) raised from x1, x2 and x3 orbital families (Contopoulos and Papayannopoulos, 1980; Binney and Tremaine, 1987) supports these shapes. The x1 orbits align with the major axis of the bar and make up the majority of the BP/X structures; the x2 and x3 orbits are oriented in the bar's minor axis, have insignificant contributions because they are prevented by the pattern speed of the bar (Athanassoula, 1992; Martinez-Valpuesta et al., 2006). The x1v1 orbit from the x1 family tree, often known as the banana orbit, demonstrates banana shapes like "$\smile$ " or "$\frown$ " when viewed from the side (Pfenniger and Friedli, 1991). It appears when $f_x : f_z = 1 : 2$, and ranked as the F class orbits with the lowest energy by Portail et al. (2015b). Its existence has been examined by many N-body simulations and orbital analysis models, originally believed to be the bedrock of the BP/X structures (Combes et al., 1990; Patsis et al., 2002b; Martinez-Valpuesta et al., 2006). Portail et al. (2015b) analysed the dominant x1 orbits generated from made-to-measure models and N-body simulations, concluded the insignificance of the x1v1 orbits in contributing to the X structure, because of their occupations in the outer part of the bar (see the navy blue region in Figure 2.6). Instead, a family of class C orbits, the brezel orbits which occur when $f_x : f_z \approx 3 : 5$, demonstrate clear X features (bottom diagram in Figure 2.6).

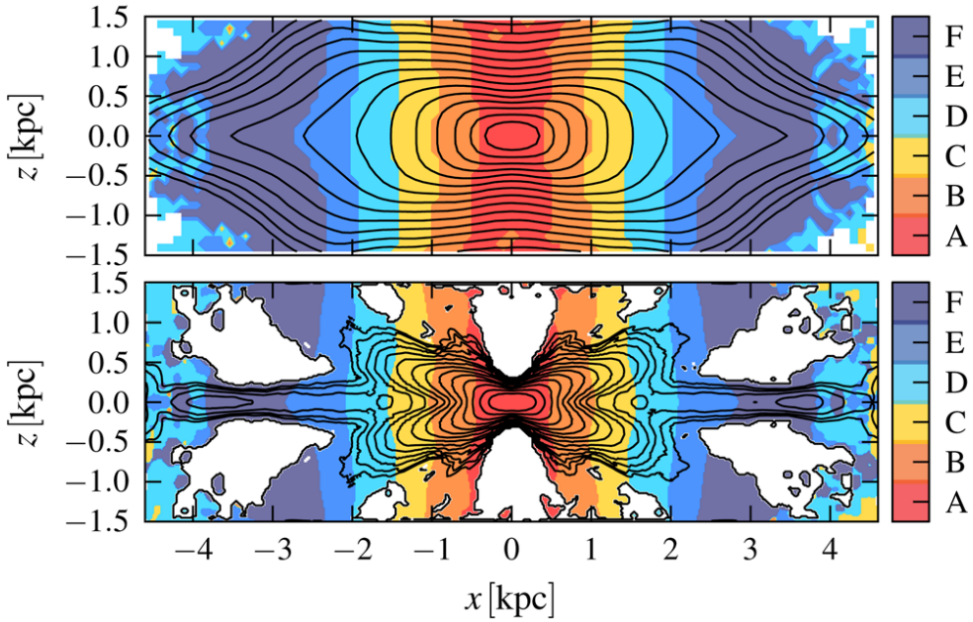

Figure 2.6: The surface density distributions of BP (top)/X (bottom) structures are presented in terms of x1 orbits, indicated by colours. Orbital classes are in alphabetic orders, following the increasing trend of $f_z : f_x$ which equals to 1.5 (A); 1.6 (B); 1.7 (C); 1.8 (D); 1.9 (E); 2.0 (F) from Portail et al. (2015b).

Abbott et al. (2017) furthered the investigation by implementing N-body simulations to mimic the x1 orbits in the MW bar. Surface mass density distribution was also applied to quantitatively measure the weighting of each orbit that contributes to the BP/X patterns. Results displayed contributions to BP structures from non-resonant boxes (which comprise 63% of bar orbits), X-tubes (8.5%) and banana orbits (3%) as well as X shapes from resonant boxlet families: fish/pretzel (5.9%) and brezels orbits (1.4%) (Abbott et al., 2017) (see Appendix). In summary, the formation of BP/X-shaped bar is a combination of orbital families; non-resonant box orbits contribute primarily to the BP shape; the resonant boxlets orbits makes up the X morphology. Currently, the connection between the bar thickening processes and the shapes of stellar orbits is still unclear. Explaining the formation of non-resonant box orbits in the bar buckling mechanisms might be the first insight into the bar formation phenomenon.

3. PROJECT OUTLINE

To create and reveal the nature of BP/X morphology, I will simulate and investigate the dynamics of stellar orbits in a slowing bar under the effect of the VLR and the MOR.

- This project was started with simple orbit simulations of stars in the McMillan (2017) potential, consisting of a disc and halo. I have adapted an existing C++ orbit simulation code with a leapfrog algorithm to track the trajectories of stars within the potential.
- What are the **characteristics of stellar orbits in an unperturbed disc**? I have been focusing on analysing the stellar orbits launched from the disc mid-plane with a Gaussian velocity distribution. To study the energy changes in the stars' orbits, I have analysed the extent of the vertical motions and the radial ranges. In Figure 3.1 (left diagram), the inclined line formed above all the points is due to the galactic potential which forbids stars to escape. Figure 3.1 (right) shows the occurrences of the MOR when the curved line breaks. This phenomenon allows the stellar orbit to exchange momentum in radial and vertical components and results in a decrease or increase of the vertical oscillation range (zmax) around such resonance.

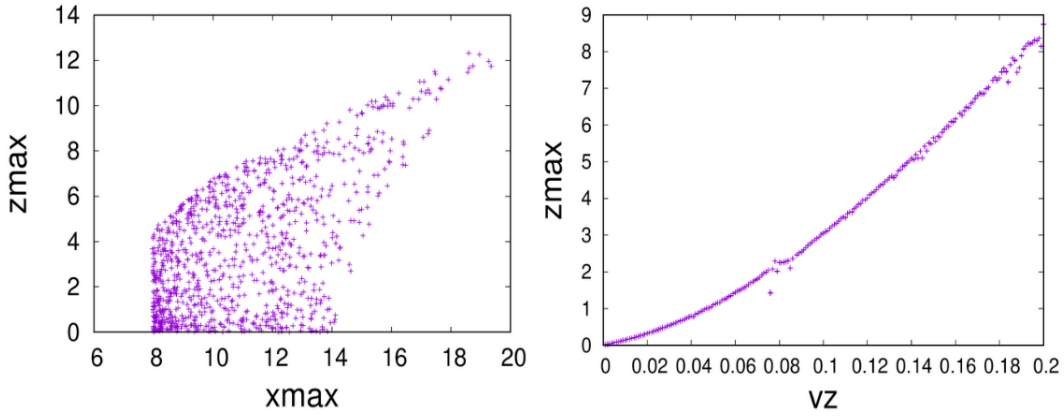

Figure 3.1: Orbits of 1000 stars in the x_{max}, z_{max} plane (left diagram) and v_z, z_{max} plane (right diagram) with initial position 8 kpc away from the centre.

- In what **disciplines** have understanding the **orbital structure and changes** benefited us? **(1)** Since the kinematics of stars in a galaxy are highly dependent on the galactic potential (left diagram of Figure 3.1), precision measurements can take place to map the in-plane and vertical potentials. **(2)** It aids with calculating and evaluating the bar's slow-down rate by the occupation in the resonance. **(3)** The dynamical history of a bar becomes clearer with the knowledge of its stellar populations and age distributions via studying stars' orbits, hence contributes to tackling the dark matter problem first posited by Oort (1932).
- The next part of the project will **simulate and analyse the stellar orbits in a slowing bar (a perturbation of the disc) and a realistic galactic bar.** See detailed goals and tasks in Table 3.1.

Time	Goals	Tasks
Oct- Nov 2020	**Understand the MOR of orbits in a disc.**	• Fourier-analysing the orbits in the disc to identify the occurrences of the MOR.
Nov 2020- Jan 2021	**Computationally model and study the formation of stellar orbits in a slowing bar via resonances.**	• Having classified motions of resonant stars that make up the disc, I will implement recipes for a slowing galactic bar and hence conduct the energy and frequency analyses. • Despite the difficulty in calculating the vertical actions, I will attempt to develop an analytical understanding of the changes in action space if time allows.
Jan- Mar 2021	**Simulate and investigate the stellar orbits within a BP/X-shaped bar in a realistic model.**	To make the simple model more realistic, I will carry out one of the following tasks: • Comparing the resulting orbits to kinematic data in the MW. • Running N-body simulations that trace the same changes.
2021- 2024	**Identify the relations of orbital shapes and the bar thickening mechanisms.**	• This project could be further pursued at PhD level by theorizing how a slowing bar, or a growing nuclear disk trap and drags the stars passed by resonances with a focus on their MOR.

Table 3.1: The timeline of my project.

BIBLIOGRAPHY

C. G. Abbott, M. Valluri, J. Shen, and V. P. Debattista. *MNRAS*, 470, 1526–1541, 2017.

E. Athanassoula. *MNRAS*, 259, 328-344, 1992.

E. Athanassoula. *MNRAS*, 341, 1179-1198, 2003.

M. Aumer and R. Schönrich. *MNRAS*, 454, 3166-3184, 2015.

J. Binney and S. Tremaine. *Galactic Dynamics*. Princeton Univ. Press, Princeton, 1987.

J. Binney and S. Tremaine. *Galactic Dynamics. 2nd edn.* Princeton Univ. Press, Princeton, 2008.

A. Brooks and C. Christensen. *Astrophys. Space Sci. Lib.*, 418, 317, 2016.

M. Bureau, G. Aronica, E. Athanassoula, J. Dettmar, A. Bosma, and K. C. Freeman. *MNRAS*, 370, 753, 2006.

R. Chiba, J. K. S. Friske, and R. Schönrich. *arXiv e-prints, arXiv:1912.04304*, 2019.

F. Combes and R. H. Sanders. *A&A*, 96, 164, 1981.

F. Combes, F. Debbasch, D. Friedli, and D. Pfenniger. *A&A*, 233, 82, 1990.

G. Contopoulos and T. Papayannopoulos. *A&A*, 92, 33, 1980.

G. Contopoulos and M. D. Weinberg. *ApJ*, 201, 566, 1975.

E. Dwek, R. G. Arendt, and et al. *MNRAS*, 445, 716, 1995.

P. Erwin and V. P. Debattista. *MNRAS*, 431, 3060, 2013.

P. Erwin and V. P. Debattista. *ApJ*, 825, L30, 2016.

H. T. Freudenreich. *ApJ*, 492, 495-510, 1998.

D. Friedli and D. Pfenniger. *Jarvis B and Terndrup D M eds and ESO/CTIO Workshop on Bulges of Galaxies ESO and Garching*, 265-268, 1990.

D. Friedli, W. Benz, and R. Kennicutt. *ApJ*, 430, L105, 1994.

O. A. Gonzalez, D. A. Gadotti, and et al. *A&A*, 591, A7, 2016.

T. G. Hawarden, C. M. Mountain, S. K. Leggett, and P. J. Puxley. *MNRAS*, 221, 41P-45P, 1986.

L. Hernquist and M. D. Weinberg. *ApJ*, 400, 80, 1992.

E. Hummel, J. M. van-der Hulst, R. C. Kennicutt, and W. C. Keel. *A & A*, 236, 333, 1990.

J. Kormendy, R. C. Kennicutt, and J. C Robert. *A&A*, 42, 603-683, 2004.

E. Laurikainen, H. Salo, R. Buta, and J. H. Knapen. *MNRAS*, 418, 1452–1490, 2011.

I. Martinez-Valpuesta and I. Shlosman. *ApJ*, 613, L29, 2004.

I. Martinez-Valpuesta, I. Shlosman, and C. Heller. *ApJ*, 637, 214, 2006.

P. J. McMillan. *MNRAS*, 465, 76, 2017.

A. McWilliam and M. Zoccali. *ApJ*, 724, 1491-1502, 2010.

D. M. Nataf and A. Udalski. *AJ*, 721, pp L28-L32, 2010.

D. M. Nataf, A. Udalski, A. Gould, and et al. *ApJ*, 721, L28, 2010.

M. Ness and D. Lang. *ApJ*, 152, 14, 2016.

J. H. Oort. *Bull. Astron. Inst. Neth.*, 6, 249–87, 1932.

P. A. Patsis and E. Athanassoula. *A&A*, 335, 1049, 2002a.

P. A. Patsis, C. Skokos, and E. Athanassoula. *MNRAS*, 337, 578, 2002b.

D. Pfenniger and D. Friedli. *A&A*, 252, 75, 1991.

M. Portail, C. Wegg, and O. Gerhard. *MNRAS*, 450, L66–L70, 2015b.

A. C. Quillen. *AJ*, 124, 722, 2002.

A. C. Quillen, I. Minchev, and et al. *MNRAS*, 437, 1284, 2014.

J. A. Sellwood. *ApJ*, 473, 733, 1996.

J. A. Sellwood and O. Gerhard. *MNRAS*, 495, 3175–3191, 2020.

J. A. Sellwood and A. Wilkinson. *Rep. Prog. Phys.*, 56, 173, 1993.

M. A. Shaw. *MNRAS*, 229, 691, 1987.

M. F. Skrutskie, R. M. Cutri, R. Stiening, and et al. *AJ*, 131, 1163, 2006.

S. Sridhar and J. Touma. *MNRAS*, 279, 1263-1273, 1996.

A. Toomre. *Geophys. Fluid Dyn.*, 66-46, 111, 1966.

S. Vásquez, M. Zoccali, and V. Hill. *A&A*, 555, A91, 2013.

M. Vera, S. Alonso, and G. Coldwell. *A & A*, 95, A63, 2016.

C. Wegg and O. Gerhard. *MNRAS*, 435, 1874, 2013.

M. D. Weinberg. *MNRAS*, 213, 451, 1985.

E. L. Wright, P. R. M. Eisenhardt, R. M. Peter, and et al. *ApJ*, 140, 1868-1881, 2010.

APPENDIX

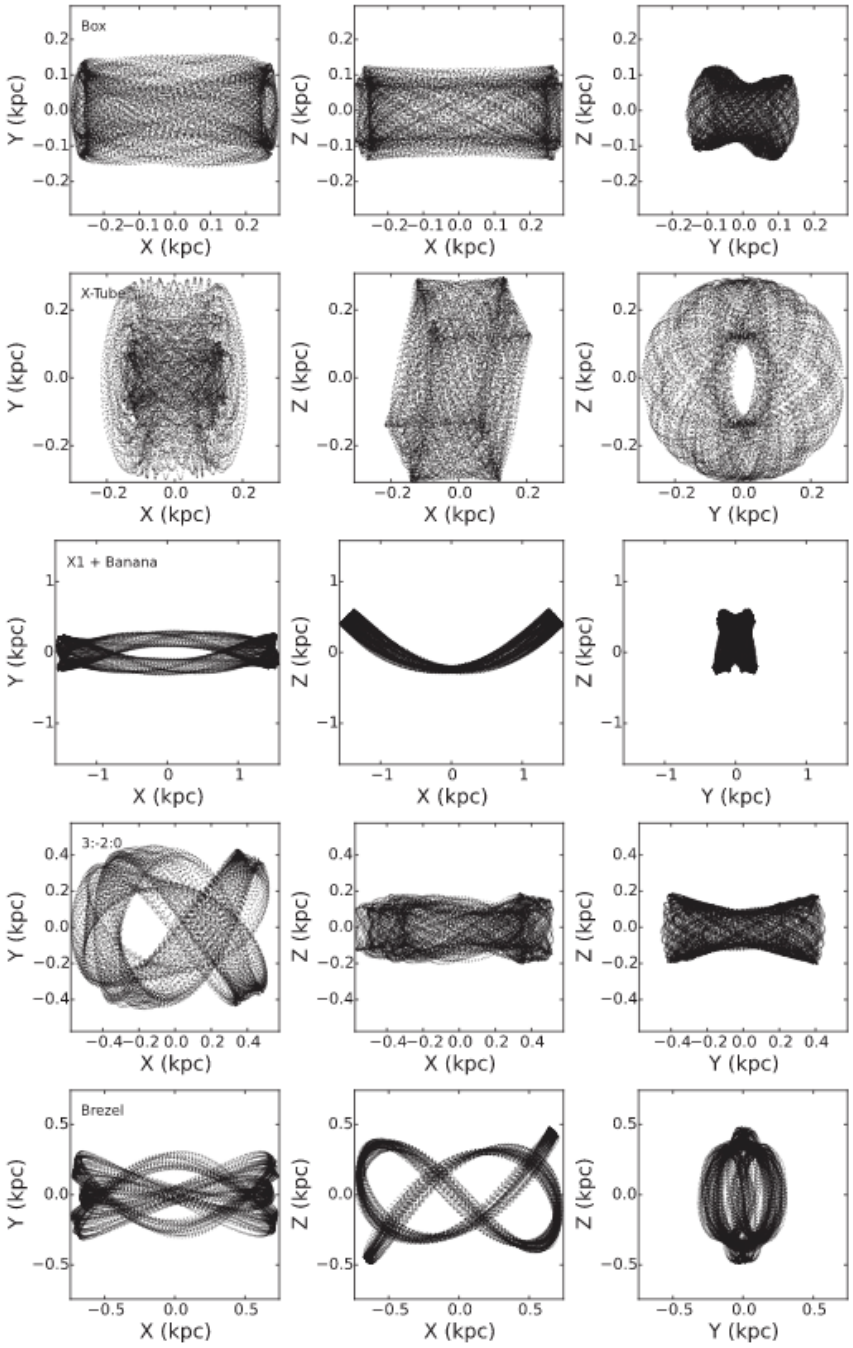

Figure 3.2: The five distinct orbital shapes from the top to the bottom are as follows: non-resonant box orbits, X-tube orbits, x1 & banana orbits (2:-2:1), fish/pretzel orbits (3:-2:0) and brezel orbits (3:0:-5) from Abbott et al. (2017).